J Mater Sci: Mater Med (2007) 18:1973–1981
DOI 10.1007/s10856-007-3125-3

The effect of physiological cyclic stretch on the cell morphology, cell orientation and protein expression of endothelial cells

Valerie Barron · Claire Brougham · Karen Coghlan · Emily McLucas · Denis O'Mahoney · Catherine Stenson-Cox · Peter E. McHugh

Received: 31 March 2006 / Accepted: 25 July 2006 / Published online: 7 June 2007

Abstract In vivo, endothelial cells are constantly exposed to pulsatile shear and tensile stresses. The main aim of this study was to design and build a physiological simulator, which reproduced homogenous strain profiles of the tensile strain experienced in vivo, and to investigate the effect of this cyclic tensile strain on the cell morphology, cell orientation and protein expression of endothelial cells. The biological response of human umbilical vein endothelial cells to a uniaxial cyclic stretch, in this newly developed simulator, was examined experimentally using immunohistostaining and confocal imaging and it was found that the cells elongated and oriented at 58.9° ± 4.5°. This value was compared to a mathematical model where it was revealed that endothelial cells would orient at an angle of 60°. This model also revealed that endothelial cells have an axial strain threshold value of 1.8% when exposed to a 10% cyclic strain at 1 Hz for 3 h. Cells cultured under conditions of cyclic strain showed increased ICAM-1 immunostaining when compared to static cells whereas, a marked decrease in the levels of VCAM-1 receptor staining was also observed. Haemodynamic stresses can modulate the endothelial cell adhesion response in vivo thus, taken together; this data validates the bioreactor as replicating the physiological environment.

V. Barron (✉) · C. Brougham · K. Coghlan · E. McLucas · D. O'Mahoney · C. Stenson-Cox · P. E. McHugh
National Centre for Biomedical Engineering Science, National University of Ireland, Galway, Orbsen Building, Galway, Ireland
e-mail: valerie.barron@nuigalway.ie

C. Brougham · K. Coghlan · P. E. McHugh
Department of Biomedical and Mechanical Engineering, National University of Ireland, Galway, Galway, Ireland

Introduction

Atherosclerotic lesion development, a hallmark of atherosclerosis, does not occur randomly within the vasculature but rather prevails at certain sites, associated with high stress and high stretch [1], such as discontinuities in the arterial trees, the branches of the coronary arteries and the carotid bifurcation. It has been hypothesised that certain mechanical factors such as pressure induced wall stress and blood flow disturbances are contributing factors to the localisation of atherosclerotic lesions [1–3].

The endothelial cell layer that lines the entire vascular system is a metabolically active monolayer that regulates a variety of biological responses and physiological functions [4, 5]. Alterations in endothelial cells, gene and protein expression, underpin a number of features characteristic of cardiovascular disease including monocyte-endothelial interactions. Due to the constant pulsatile blood flow through the circulatory system, endothelial cells are constantly exposed to a shear and tensile stress [6]. Various in vitro investigations have examined these mechanical stresses both independently and in combination [7–13]. However, these studies have been carried out on endothelial cells from a variety of sources using a wide range of physiological parameters, including various physiological testers, frequencies and strain rates. Due to inconsistent testing materials and methods, it is difficult to compare and extrapolate the results obtained from one experimental study to another.

Although the biological response of endothelial cells subjected to shear stresses from fluid flow has been extensively studied, the biological response of endothelial cells on deformable substrates subjected to cyclic tensile strain still requires further characterisation. To date, many of the studies seed cells on circular substrates to which a

vacuum is applied [14–16]. A drawback of such studies would seem to be that the cells are exposed to a heterogeneous strain field with minimum strain at the centre of the membrane and a maximum strain at the periphery. Cell morphology and cell orientations observed on these circular substrates tend to be quite heterogeneous due to the nature of the strain applied [7, 14, 15]. The suitability of such an approach for simulating the strain field experienced by cells lining an artery is questionable, in particular for highly cylindrical segments of artery.

This study aims to address some of these issues by employing finite element analysis (FEA), biomechanical engineering principles and biological techniques. Using FEA, the strain profile of circular substrates previously studied [7, 14, 15] was evaluated and compared to that generated by rectangular strip substrates subjected to cyclic tension. This analysis quantifies the strain heterogenity inherent in the circular substrate approach and identifies the design criteria required to expose endothelial cells to in - vivo levels of pulsatile strain. Using this information a physiological simulator was designed and built to house rectangular substrates. Upon optimisation of the mechanical requirements, the biological response of endothelial cells was examined using immunohistostaining techniques. To validate the system, cell orientation was compared to the results of other experimental studies [17–21], and to the predications of a mathematical model described by Wang et al. [13]

In their study Wang et al. [13] proposed a mathematical model to predict the orientation response of cells grown on a substrate which was cyclically stretched. This model is based on the hypothesis that for each cell type there is an axial strain limit or threshold value above which few cells are found, and that this axial strain threshold is normally distributed within the cell population. Wang et al. [13] proposed the Green Strain diagram to predict the peak cell orientation angle based on the axial strain the cell experiences. For melanocytes, Wang et al. [13] predicted an orientation angle of 60° with a threshold stain limit of 3.5% and a standard deviation of 1.0% around this peak value of 60°. This model was further explored up by Neidlinger-Wilke et al. [22] who found an axial strain limit of 6.4% for osteoblasts and 4.2% for fibroblasts. In this study, an axial strain limit for endothelial cells is identified by matching the observed experimental reorientation response in the physiological simulator with the predicted reorientation response of this mathematical model.

It has also been shown, in shear stress studies, that protein expression of endothelial cells in the coronary artery is regulated by shear. However, to date, there is very little information on the role of pulsatile tensile stress. In the present study, immunostaining of the adhesion molecules; ICAM-1 and VCAM-1, were examined using confocal scanning calorimetry and semi-quantitative imaging techniques.

Materials and methods

Finite element analysis

Models of a previously used circular silicone substrate and a newly developed rectangular planar substrate were analysed using ABAQUS software (Version 6.4) under the assumptions of large strain kinematics. The circular substrate was modelled as axisymmetric and only the upper right quadrant of the rectangular substrate was modelled in the plane due to symmetry. Eight-noded hyperelastic Neo-Hookean rectangular elements were chosen for both analyses. The material was considered as having a Poisson's ratio of 0.45, and was assigned appropriate initial bulk modulus and initial shear modulus values corresponding to an equivalent Young's modulus of 900 kPa.

The circular substrate model had diameter of 34.5 mm and 0.5 mm thickness. A zero displacement/rotation boundary condition was applied on the vertical circumferential axis of the substrate and 100 steps of negative pressure of 0.0061 kPa were applied incrementally to the bottom surface of the substrate for a total of 0.61 kPa. This particular pressure was chosen to displace the silicone substrate so as to achieve a 10% strain at the centre, which is reflexive of the strains applied in vitro [13, 16, 23]. A diagram of the deformed model is shown in Fig. 1a.

The rectangular substrate model, which was 80 mm in length, 25 mm in width and 1 mm thick, was subjected to longitudinal uniaxial stretching in the plane. Only the upper right quadrant was modelled and symmetry boundary conditions were applied along the bottom edge of this quadrant. The top edge was left free. A uniform longitudinal displacement was applied to the left edge nodes to deform the substrate 10% of its original length in the longitudinal direction, while transverse displacements of this edge were unconstrained. The right edge of the quadrant was fully constrained in the longitudinal and transverse directions to simulate clamping.

Following the FE analysis, the nodal displacements for the two models were obtained and strain profiles were calculated. For the circular model the strain components ε_{xx}, ε_{yy} and ε_{xy} were generated by ABAQUS and averaged for each element on the top surface (upon which the cells would be seeded). The orientation of each top surface element, θ_d (see Fig. 1a), was determined from the top surface nodal displacements. Based on θ_d, the radial strain ε_r for each element was then determined from ε_{xx}, ε_{yy} and ε_{xy} using standard tensor rotation formulae. The circumferential strain, ε_c, was calculated using the circumferential

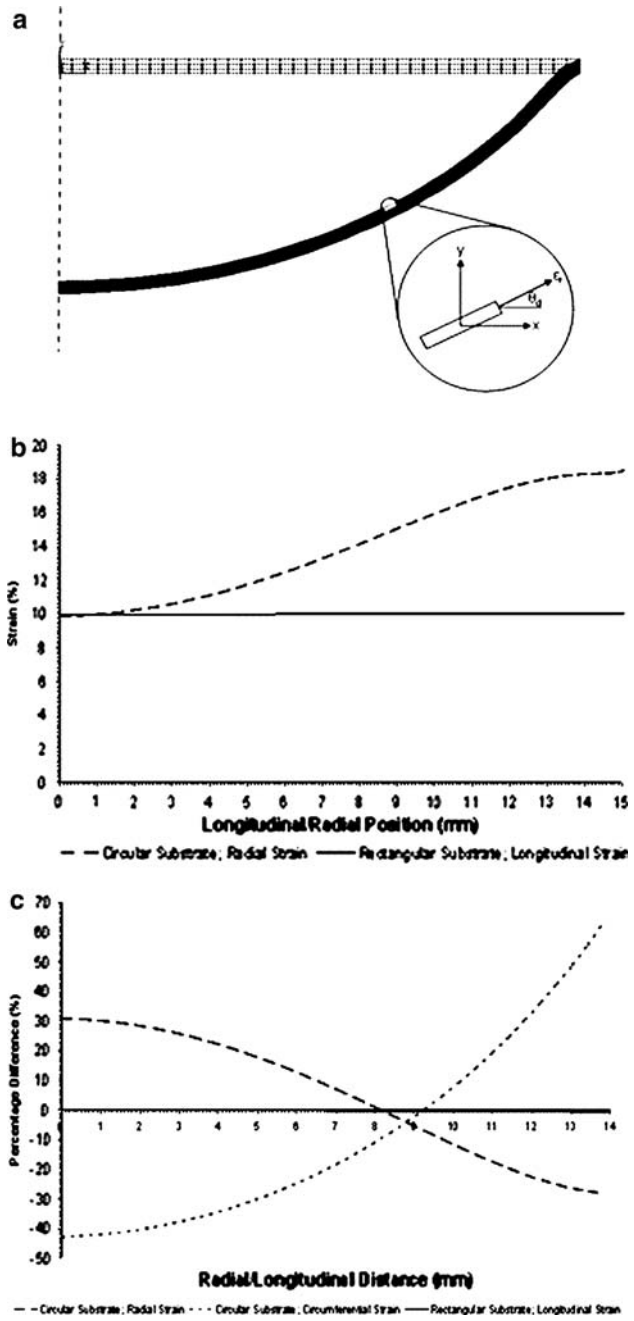

Fig. 1 (**a**) Deformed circular substrate with emphasis on a single element along the top surface to show the orientation, θ_d, of the element and the radial strain, ε_r, tangential to the top surface of the substrate. (**b**) Dramatically varying radial strain distribution for the circular substrate compared to consistent strain distribution for the rectangular substrate. The origin of the longitudinal and radial positioning is mid-length of the rectangular substrate and at the centre of the circular substrate respectively. (**c**) Percentage difference of the actual strains compared to the average strain across the circular and rectangular substrates. The average radial stain and circumferential strain for the circular substrate were 14.27% and 7.4% and the average strain for the rectangular substrate was 9.96%. The origin of the longitudinal and radial positioning is mid-length of the rectangular substrate and at the centre of the circular substrate respectively

stretch ratio method, as used in Gilbert et al. [24]. In the axisymmetric model the horizontal position for each node on the top surface defines the circumference of a circle. The ratio of the new circumferential length following deformation to the undeformed circumferential length defines the stretch ratio λ_c. From this ε_c is determined through

$$\varepsilon_c = 0.5\,(\lambda_c^2 - 1) \tag{1}$$

For the rectangular model, the longitudinal elemental strain was averaged across the width of the substrate for each transverse row of elements, resulting in a measure of longitudinal strain as a function of longitudinal distance from the centre of the substrate toward the clamped edge.

An analysis of the deformation of a circular substrate has been performed by Gilbert et al. [24] using a Mooney-Rivlin material description. Inhomogeneous strain profiles were generated, however no explicit definition of radial strain in the deformed configuration was given. In the present analysis, a radial strain in the deformed configuration is explicitly defined and quantified; radial strain is interpreted as the strain component in a plane containing the axis of symmetry of the substrate, in a direction tangential to the top surface of the substrate (Fig. 1a), i.e., the radial component of strain that the cells experience.

The results of the FEA performed here for the circular substrate revealed a strong gradient of strain in both the radial and circumferential directions. By contrast, the strain profile for the rectangular substrate was consistent across the whole surface, thereby providing an appropriate strain field for cell stimulation, analogous to the strain experienced by endothelial cells in vivo. The graph in Fig. 1b shows the strain profiles for both of the modelled substrates. The radial strain for the circular substrate varies dramatically from 10% at the centre up to 19% at a radius of 15 mm, beyond which there is a very steep rise towards the periphery due to the clamped edge. This profile differs from that presented by Gilbert et al. for radial strain, with the results here showing a more severe radial strain gradient. The strain profile for the rectangular substrate is consistent at 10%, only dropping slightly at the outside edge due to the clamping. The circumferential strain for the circular substrate was also seen to vary significantly. The plot in Fig. 1c shows the percentage difference between the actual strains for the substrates and the average strains for the substrates. The circumferential strain varied from –42% up to 62% and the radial strain from –28% to 31% compared to less than 2% for any point on the rectangular substrate.

Due to the strong heterogeneity in substrate strain exhibited by the circular substrate, it was decided to develop the physiological simulator based on the principle

of the stretching of a rectangular substrate, that results in much more favourably homogeneous strain states that can lead to far more meaningful experimental test results.

Design and development of physiological simulator

The basic working principle of the physiological simulator developed to evaluate endothelial cell response to uniaxial cyclic stretching is shown in Fig. 2. It consists of a surface modified rectangular silicone substrate, seeded with cells, which is clamped at both ends. Strain is applied by the systematic and accurate movement of one of the clamps, relative to the other fixed clamp, along the long axis of the silicone membrane.

The rig itself was made from PMMA, a biocompatible transparent material that allowed visualisation of the test. The fixed grip of the rig (316L stainless steel) was designed so that it was self-tightening upon loading and would not loosen during testing. The rig was mounted into the environmental chamber of an Instron 8,874 tensile testing machine, where cyclic conditions were applied to the cell seeded silicone substrate in a precisely controlled, recordable and repeatable manner. The environmental chamber provided the required physiological conditions during the test. All materials used were tested for biocompatibility and had no adverse cytotoxic effects on HUVECs.

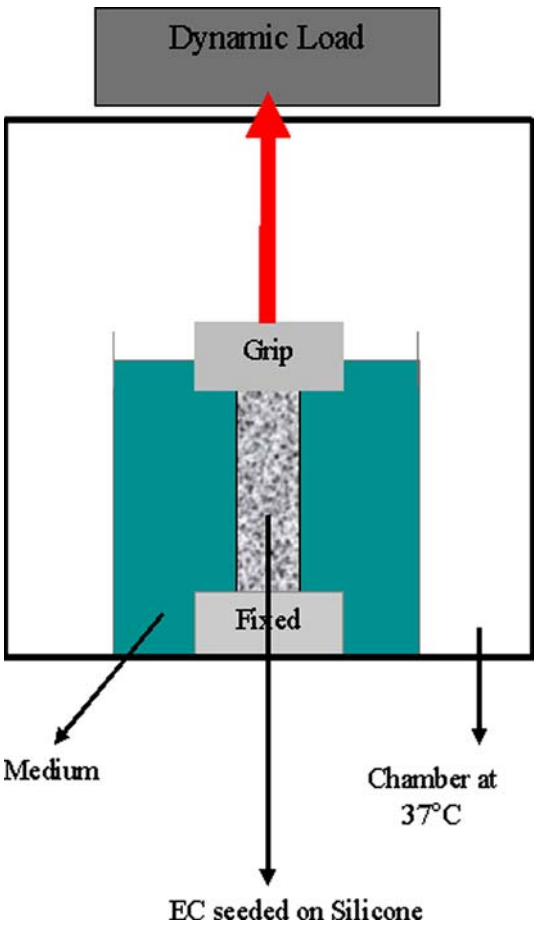

Fig. 2 Schematic diagram of purpose-built mechano-transduction rig

The substrate upon which the cells are seeded plays a very important role when applying the cyclic stretch. The chosen substrate has to be elastic in the region subjected to cyclic stretch, be biocompatible, non-toxic to vascular cells and have suitable surface properties for efficient cell attachment. The material used in this study was a commercially available silicone elastomer (Goodfellow, U.K.). Prior to cell seeding, silicone substrates were washed with ethanol and sonicated in distilled water for 20 min. Then the strips were plasma treated in air for 10 min using 150 Watts in a Europlasma Junior Plasma Treatment chamber followed by sterilisation using an ultra violet source for 1 h.

Cell culture

Studies were performed using human umbilical vein endothelial cells (HUVECs) obtained from Cambrex, UK. Cells were maintained in HUVEC EGM-2 Bullet kit media (Cambrex, UK). Cells were propagated at 37 °C, in a humidified environment with a 5% CO_2 air atmosphere and were used at passages 3–9. The cells were seeded onto the strips at a density of 40,000/cm^2 under sterile conditions. After 24 h, the silicone substrates were subjected to a 10% cyclic strain at a frequency of 1 Hz for 3 h in phosphate buffered solution at 37 °C. Following removal from the physiological simulator, a mark was placed on the uppermost part of the strip to indicate the direction of imposed stretch. This was obvious during all further analysis and used as an indicator of direction throughout the follow up analysis. Furthermore the rectangular dimensions of the strip within the simulator ensured that the cell could only be stretched along the longitudinal axis allowing the direction of stretch to be known. Control strips were subjected to a 0% strain under identical conditions. The sampling process for the statistical analysis involved selecting regions containing at least 50 cells with few cell–cell interactions [22].

Cell response

Differential staining was used to examine cell morphology and orientation. Cells were fixed in methanol for 15 s prior to being stained with Eosin for 15 s and haematoxylin for 15 s. Samples were washed with H_2O and images were captured using light microscopy as seen in Fig. 3.

For immunostaining, all samples were treated by washing in a PBS (1%) BSA solution and then fixed with a (4%) paraformaldehyde (2%) sucrose solution for 5 min at

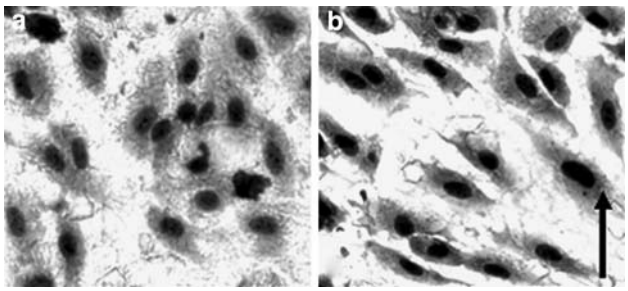

Fig. 3 Phase contrast images of differentially stained cells showing. (**a**) random distribution of control cells on plasma treated silicone with 0% strain, (**b**) aligned cells on plasma treated silicone cyclically stretched at 1 Hz by 10% for 3 h. The arrow indicates direction of applied stretch

room temperature followed by a further three rinses with PBS/BSA. For ICAM-1 and VCAM-1 visualisation, separate samples for each were stained with FITC-conjugated mouse anti-human ICAM-1 and VCAM-1 monoclonal antibodies (TCS Cellworks, UK) for 60 min at room temperature followed by further washing with PBS/BSA. Endothelial cells cultured under static conditions, fixed and stained with anti-FITC mouse secondary antibody alone comprised the negative control for antibody specificity. The cells did not exhibit immunoreactivity. In order to stain for actin filaments staining a fluorescent conjugate of phalloidin (Molecular Probes, UK) was used; cells were permeablised prior to fixing using buffered Triton x-100 solution for 5 min at 0 °C. The samples were stained with phalloidin solution for 20 min at room temperature and washed in ice-cold PBS/BSA three times. To stain the nucleus, a 5 μg/mL solution of propidium iodide (Molecular Probes, UK) was added to fixed cells for 5 min, followed by three washes with PBS/BSA.

Subsequently, semi-quantitative analysis of ICAM-1 and VCAM-1 protein expression levels was conducted using Image Pro® Plus analysis software (Media Cybernetics, UK). This software accurately measures the number of pixels of green fluorescence emitting from the bound FITC-conjugated antibody in each sample which has bound to the relevant adhesion molecule in each cell. Samples were normalised against the global background fluorescence and all images were assessed at the same magnification. Experiments using this method were conducted in triplicate and a standard error of mean was determined for both stretched and control cells.

All cell lines were tested for the endothelial cell specific marker, von Willebrand factor, using polyclonal rabbit anti-human von Willebrand factor (Dakocytokine, UK), after testing was complete. Some cells which had undergone seeding on the silicone strips and strain in the physiological simulator were trypsinised and grown again under normal tissue culture conditions to see if the silicone elicited any adverse effects which were not immediately apparent. These cells were also tested with von Willebrand factor and showed no signs of differentiation.

Cell orientation

The angle of orientation was determined by manually tracing the perimeter of each cell and drawing the major axis of the acquired shape and measuring the angle between the major axis and the baseline, represented by the stretching direction. The acute angle between the perpendicular baseline and the major axis of the cell was recorded and all results were between 0° and 90°. An angle of 0° was indicative of a cell aligned perfectly parallel to the stretching direction, while an angle of 90° was indicative of the cell aligned perfectly perpendicular to the stretching direction. From these cell orientation measurements, cell orientation frequency distributions were calculated in 5° intervals.

Mathematical model

In this study, the same techniques developed by Wang et al. [13] were employed to find the axial strain threshold limit and corresponding predicted range of orientation angles, for endothelial cells, at 10% applied strain. Wang et al. [13] demonstrated that cells respond to strain magnitude along their major axis, as opposed to the principle applied strain direction (or the substrate direction). Wang et al.'s theory was that each cell has an axial strain threshold, and reorientation is a cellular response which tries to reduce the cells' axial strain below its threshold value. It is assumed that within a cell population, the threshold values follow a normal distribution about some mean value (also termed the axial strain limit) and standard deviation.

In the Wang et al. [13] model, the substrate in considered to lie in the x–y plane, where x is the longitudinal, or stretch, direction. Consider a cell whose major axis makes an angle θ with the positive x-axis. Using the definition of Green Strain, as detailed in [13], the following relationship (Eq. (2)) can be established between θ and the axial strain that the cell experiences, $\overline{\varepsilon_{aa}}$, where v is the Poisson's ratio of the substrate and δ_x is the applied engineering strain in the x-direction. In the model this relationship is used to establish cell orientation limits for a given cell axial strain threshold, $\overline{\varepsilon_{Th}}$.

$$\theta = \cos^{-1}\left(\sqrt{\frac{2(\overline{\varepsilon_{aa}}/\delta_x) + (2v - v^2)\delta_x}{2(1+v) + (1-v^2)\delta_x}}\right) \tag{2}$$

This model, which was implemented using MS Excel, uses a random generation of numbers (in a normal distribution) as an example of a population (n = 500) of cell thresholds. For each threshold value, a range of cell orientations, where the axial strain along the cell's major axis is below the threshold, was computed. Using Eq. (3) a random orientation for each cell was generated, within the confines of the range of possible orientations for that cell threshold value.

$$\theta = \theta_a + u\,(\theta_b - \theta_a) \tag{3}$$

where u is a uniformly distributed random number between 0 and 1. θ_a and θ_b are the angles which define the permitted range of orientations for a given cell threshold value. Three cases exist which are visualised on the Green strain diagram shown in [13]. The range of orientations permitted within case 1 is characterised by $|\overline{\varepsilon_{Th}}| > |\overline{\varepsilon_{xx}}|$, where, θ_a = 0° and θ_b = 90° and where $\overline{\varepsilon_{xx}}$ is the Green Strain in the x-direction. The range for case 2 is $|\overline{\varepsilon_{yy}}| < |\overline{\varepsilon_{Th}}| < |\overline{\varepsilon_{xx}}|$, where θ_a is found by substituting $\overline{\varepsilon_{Th}}$ for $\overline{\varepsilon_{aa}}$ in Eq. (2) and θ_b is 90° and $\overline{\varepsilon_{yy}}$ is the Green Strain in the y-direction. Finally, case 3 has a range $|\overline{\varepsilon_{Th}}| < |\overline{\varepsilon_{yy}}|$ where both θ_a and θ_b are found through Eq. (2).

The percentage frequency of occurrence of the generated orientations in 5° intervals was computed. Through changing the mean and standard deviation of the strain threshold distribution, the best fit to experimental data was obtained. This was statistically confirmed using the method of least squares.

Results

Cell morphological response

From the images in Fig. 3a it can be seen that the control cells subjected to 0% stretch were randomly oriented and had rounded cobblestone morphology. However, the cells subjected to 10% cyclic stretch (Fig. 3b) were seen to elongate and realign obliquely to the direction of stretch.

This is further evidenced in the propidium iodide stained CLSM images (Fig. 4), where it can be seen that the nuclei of the control cells were randomly oriented (Fig. 4a), while Fig. 4b reveals that the nuclei of the mechanically conditioned cells begin to elongate and realign at an angle to the direction of stretch.

Furthermore, phalloidin staining of the endothelial cells demonstrated a similar response to the imposed cyclic stretch. Compared to the randomly oriented control cells which were not subjected to strain (Fig. 5a), the strained cells oriented obliquely to the direction of stretch, as shown in Fig. 5b. The phalloidin staining shows how the cytoskeleton has elongated as a result of the straining.

Cell orientation response

The orientation angles of the control cells which were exposed to 0% stretch were found to be highly random (Fig. 6a). In contrast, cells subjected to the biomechanical stimulus orientated obliquely towards the direction of stretch. The mean orientation angle of measured cells was

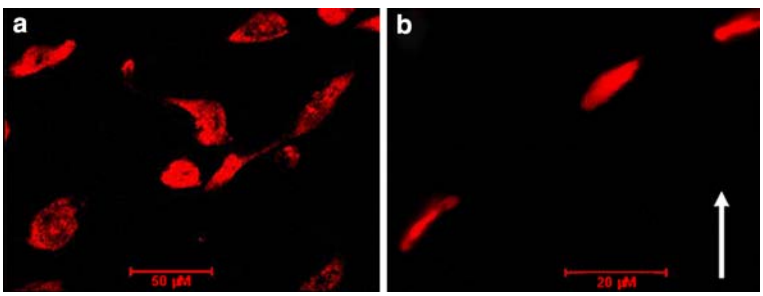

Fig. 4 CLSM image of propidium iodide stained nuclei of (**a**) randomly orientated control cells on plasma treated silicone with 0% strain (**b**) aligned cells on plasma treated silicone cyclically stretched at 1 Hz by 10% for 3 h. The arrow indicates direction of applied stretch

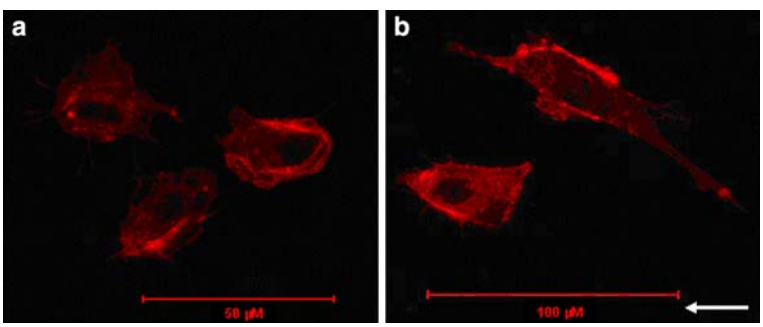

Fig. 5 CLSM image of phalloidin stained actin fibres of (**a**) randomly orientated control cells on plasma treated silicone with 0% strain (**b**) cells on plasma treated silicone cyclically stretched at 1 Hz by 10% for 3 h. The arrow indicates direction of applied stretch

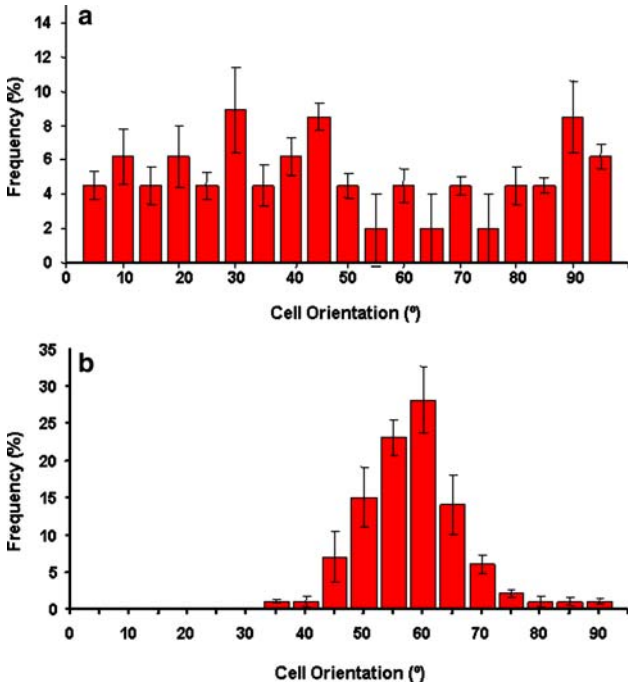

Fig. 6 Experimental observation of cell orientation for (**a**) control cells on plasma treated silicone with 0% strain (**b**) cells on plasma treated silicone, cyclically stretched at 1 Hz by 10% for 3 h. Error bars represent standard error of the mean (sem) (n = 5)

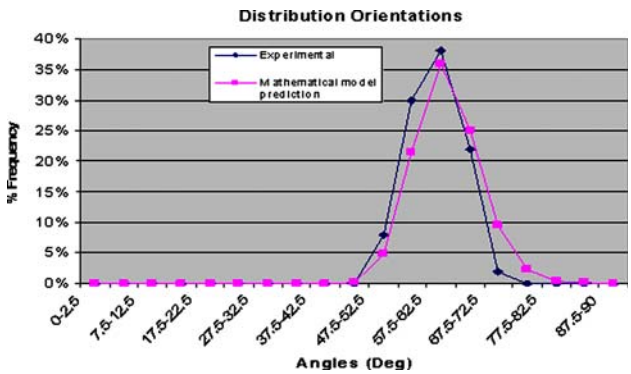

Fig. 7 Graph showing correlation between predicted and experimental orientation angle results for cyclically stretched endothelial cells

58.99° ± 4.5°. All cells measured had angles in the range 47.5–67.5° to the stretching direction (Fig. 6b). As discussed previously, the cytoskeleton of the cells has also reoriented in the direction of imposed stretch.

Comparison with mathematical model

The model was run for numerous different normal distributions of strain thresholds, with means ranging from 0.5% to 3.5% and standard deviations ranging from 0.5% to 2.5% within each of these means. Each of these curves was generated six times, for each combination of mean and standard deviation, to eliminate noise and subsequently an average curve was generated to fully represent that data set. In turn, each data set was compared with the experimental data set using the method of least squares. The combination which most closely matched the experimental data is shown in Fig. 7 and has a mean of 1.8% and a standard deviation of 0.75%. This suggests, based on the current experiment, a mean axial strain limit of 1.8% for endothelial cells.

Protein expression

A significant increase in ICAM-1 immunostaining was observed in cells exposed to cyclic stretch when compared to static culture as visualised by CLSM (Fig. 8a, b) and as further analysed by Image Pro® Plus software (Table 1). In contrast, a marked decrease of VCAM-1 immunostaining was recorded in stretched cells when compared to control cultures using the same analytical techniques (Fig. 9a, b and Table 1).

Table 1 Relative levels of adhesion molecule immunostaining

Cyclic strain	ICAM-1	VCAM-1
0%	7.2 ± 2.5%	7.8 ± 1.6
10%	14.5 ± 2.2%	3.5 ± 0.5

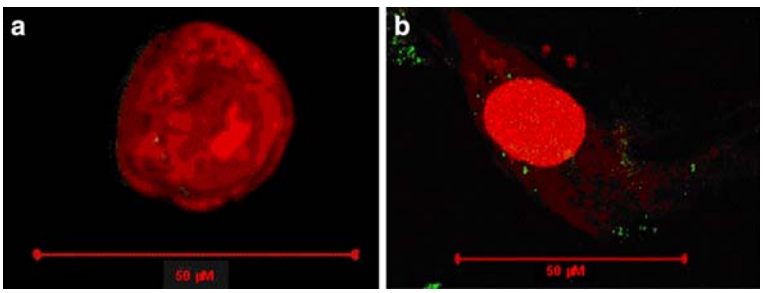

Fig. 8 Green Fluorescence Expression of ICAM-1 for (**a**) control cells on plasma treated silicone with 0% strain (**b**) cells on plasma treated silicone cyclically stretched at 1 Hz by 10% for 3 h. *Note*: Red fluorescence is propidium iodide staining for nucleus

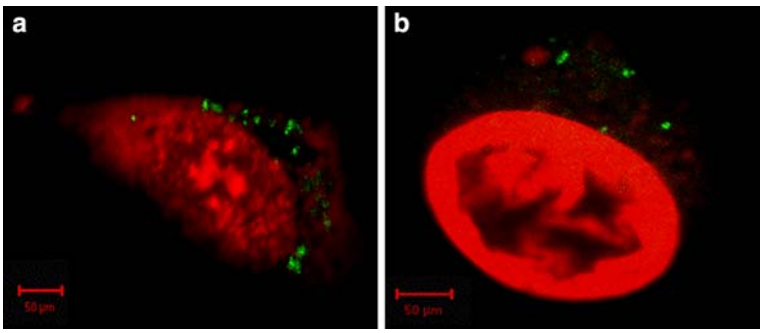

Fig. 9 Green Fluorescence Expression of VCAM-1 for (**a**) control cells on plasma treated silicone with 0% strain (**b**) cells on plasma treated silicone cyclically stretched at 1 Hz by 10% for 3 h. *Note*: Red fluorescence is propidium iodide staining for nucleus

Discussion

In this study, FEA, biomechanical design, biological techniques and a mathematical model were employed to design and utilise a physiological simulator to mimic the pulsatile stretch conditions observed in the coronary artery. This rig was used to expose endothelial cells, which were successfully cultured on modified silicone substrates, to homogeneous cyclic stretching similar to that found in the native artery.

Upon exposure to physiological levels of stretch for 3 h the endothelial cells elongated and oriented at an angle of 58.9° ± 4.5°, which is in good agreement with other experimental observations [18, 20].

Wang et al. [13] suggested that this cell orientation response could be explained by the cells attempting to reduce their axial deformation to a level below their axial strain threshold. Yamada et al. echoed that sentiment on a subcellular level proposing that stress fibers align in the direction of minimum strain to achieve minimum length change of the stress fiber [25]. Wang et al. [13] used their mathematical model to reveal that melanocytes have a mean axial strain threshold of 3.5%, above which few cells are found. In a separate study, Neidlinger-Wilke et al. [22] used a similar model and found a strain threshold of 6.4% for osteoblasts and 4.2% for fibroblasts. Using the model here, it was revealed that endothelial cells have an mean axial strain threshold of 1.8% when exposed to physiological levels of strain.

From this one could suggest that endothelial cells are easier to reorient and to elongate than these other cell lines due to their lower strain threshold. Some reports have suggested that the reorientation response of cells is the formation of a new 2-d polarity, rather than a rotation of the cell axis [26]. Endothelial cells have a round cobblestone morphology, whereas osteoblasts, fibroblasts and melanocytes are elongated and polarised in vitro. As endothelial cells are less polarised than the other cell lines discussed, it is easier for them to assume the new direction. This would explain the lower energy level required to reorient this cell line.

Another factor in the low mean axial strain threshold limit for endothelial cells could be the attributed to the dynamic conditions these cells experience in vivo. Endothelial cells are in a very dynamic environment in vivo. In contrast, osteoblasts are in a relatively static environment. While osteoblasts experience a level of shear stress from bone fluid [27] it is significantly lower than the rate and the magnitude experienced by endothelial cells. Endothelial cells are also subjected to a change of fluid fields in vivo due to vasodilation and vasoconstriction. Endothelial cells by their very function, must be very adaptable in vivo in order to maintain the phenotype of the cells and the tone of the vessels [4]. Thus, this could explain why it is easier to reorient endothelial cells than it is osteoblasts.

Previous studies suggested that the reorientation response of the cell may have an effect in inducing gene expression [28] and in directing cellular mRNA levels and protein synthesis [29, 30]. Application of shear stress to cells in vitro has been shown to regulate the expression of adhesion molecules including vascular cell adhesion molecule-1 (VCAM-1) and intercellular adhesion molecule-1 (ICAM-1) [4, 7, 31–33]. In contrast to shear stress, the effect of cyclic tensile stretch on the expression of adhesion molecules in endothelial cells is less defined. Evidence from other studies suggests a selective sensitivity of endothelial cells adhesion molecules to cyclic radial strain applied in vitro [14, 16]. Here we found that while VCAM-1 immunostaining decreased in endothelial cells subjected to the heterogeneous radial strain profiles discussed earlier, there was an induction in ICAM-1 immunostaining for these cells compared to cells cultured under static conditions [14]. In conclusion, we have designed and created a novel physiological simulator capable of reproducing strain profiles of the tensile strains found in vivo and have examined their effects upon primary endothelial cell morphology, orientation and protein expression.

Acknowledgments This work was supported by the Programme for Research in Third Level Institutions (PRTLI), administered by the Higher Education Authority (HEA), Science Foundation Ireland and the Embark Initiative, operated by the Irish Research Council for Science, Engineering and Technology (IRCSET). The authors would

like to acknowledge the help and support of Dr Bruce P. Murphy, Dr Margaret O'Brien, Dr. Michael Ball, Dr Eadaoin Timmins, Mr William Brennan and Mr. Ken Pascal, National Centre for Biomedical Engineering Science, National University of Ireland, Galway, Ireland.

References

1. B. E. SUMPIO, *J. Vasc. Surg*. **13** (1991) 744
2. S. Z. ZHAO, B. ARIFF, Q. LONG, A. D. HUGHES, S. A. THOM, A. V. STANTON and X. Y. XU, *J. Biomech*. **35** (2002) 1367
3. M. J. THUBRIKAR and F. ROBICSEK, *Ann. Thorac. Surg*. **59** (1995) 1594
4. J. N. TOPPER and M. A. GIMBRONE, Jr., *Mol. Med. Today* **5** (1999) 40
5. T. BACHETTI and L. MORBIDELLI, *Pharmacol. Res*. **42** (2000) 9
6. C. STENSON-COX, V. BARRON, B. P. MURPHY, P. E. MCHUGH and T. SMITH, *Curr. Genomics*. **5** (2004) 287
7. B. P. CHEN, Y. S. LI, Y. ZHAO, K. D. CHEN, S. LI, J. LAO, S. YUAN, J. Y. SHYY and S. CHIEN, *Physiol. Genomics* **7** (2001) 55
8. P. F. DAVIES, *Physiol. Rev*. **75** (1995) 519
9. P. F. DAVIES, K. A. BARBEE, M. V. VOLIN, A. ROBOTEWSKYJ, J. CHEN, L. JOSEPH, M. L. GRIEM, M. N. WERNICK, E. JACOBS, D. C. POLACEK, N. DEPAOLA and A. I. BARAKAT, *Annu. Rev. Physiol*. **59** (1997) 527
10. S. LEHOUX and A. TEDGUI, *J. Biomech*. **36** (2003) 631
11. X. LI and Y. FAN, *Sheng Wu Yi Xue Gong Cheng Xue Za Zhi* **20** (2003) 555
12. N. RESNICK, H. YAHAV, A. SHAY-SALIT, M. SHUSHY, S. SCHUBERT, L. C. ZILBERMAN and E. WOFOVITZ, *Prog. Biophys. Mol. Biol*. **81** (2003) 177
13. H. WANG, W. IP, R. BOISSY and E. S. GROOD, *J. Biomech*. **28** (1995) 1543
14. J. K. YUN, J. M. ANDERSON and N. P. ZIATS, *J. Biomed. Mater. Res*. **44** (1999) 87
15. B. L. RISER, S. LADSON-WOFFORD, A. SHARBA, P. CORTES, K. DRAKE, C. J. GUERIN, J. YEE, M. E. CHOI, P. R. SEGARINI and R. G. NARINS, *Kidney Int*. **56** (1999) 428
16. J. J. CHENG, B. S. WUNG, Y. J. CHAO and D. L. WANG, *Hypertension* **28** (1996) 386
17. T. TAKEMASA, T. YAMAGUCHI, Y. YAMAMOTO, K. SUGIMOTO and K. YAMASHITA, *Eur. J. Cell Biol*. **77** (1998) 91
18. J. H. WANG, P. GOLDSCHMIDT-CLERMONT, J. WILLE and F. C. YIN, *J. Biomech*. **34** (2001) 1563
19. J. H. WANG and E. S. GROOD, *Connect. Tissue Res*. **41** (2000) 29
20. M. MORETTI, A. PRINA-MELLO, A. J. REID, V. BARRON and P. J. PRENDERGAST, *J. Mater. Sci. Mater. Med*. **15** (2004) 1159
21. R. C. Buck, *Exp. Cell Res*. **127** (1980) 470
22. C. NEIDLINGER-WILKE, E. S. GROOD, J.-C. WANG, R. A. BRAND and L. CLAES, *J. Orthop. Res*. **19** (2001) 286
23. X. M. LIU, D. ENSENAT, H. WANG, A. I. SCHAFER and W. DURANTE, *Febs. Lett*. **541** (2003) 52
24. J. A. GILBERT, P. S. WEINHOLD, A. J. BANES, G. W. LINK and G. L. JONES, *J. Biomech*. **27** (1994) 1169
25. H. YAMADA, T. TAKEMASA and T. YAMAGUCHI, *J. Biomech*. **33** (2000) 1501
26. K. NARUSE, T. YAMADA and M. SOKABE, *Am. J. Physiol*. **274** (1998) H1532
27. S. C. COWIN, *J. Biomech*. **32** (1999) 217
28. M. B. DANCU, D. E. BERARDI, J. P. VANDEN HEUVEL and J. M. TARBELL, *Arterioscler. Thromb. Vasc. Biol*. **24** (2004) 2088
29. W. CARVER, M. L. NAGPAL, M. NACHTIGAL, T. K. BORG and L. TERRACIO, *Circ. Res*. **69** (1991) 116
30. D. Y. LEUNG, S. GLAGOV and M. B. MATHEWS, *Science* **191** (1976) 475
31. P. I. LELKES, C. S. KETTLUN, J. WIGBOLDUS and G. M. RUBANYI Signalling mechanisms involved in endothelial cell activation by perturbed flow. INABIS Symposium, (1998)
32. E. A. SPRAGUE, S. MOHAN, L. BALLOU and R. M. NEREM Pathways mediating low shear stress-induced vascular endothelial gene activation INABIS Symposium (1998)
33. M. YOSHIGI, E. B. CLARK and H. J. YOST, *Cytometry* **55A** (2003) 109